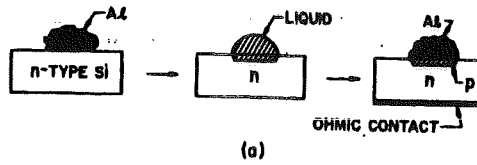


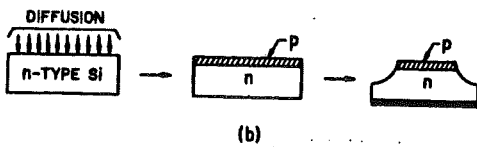
PREPARAZIONE GIUNZIONE P-N

a) LEGA
depos. Al
heating 580°C



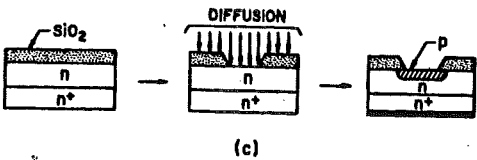
$\rightarrow \text{AuSb} + 600^{\circ}\text{C } n^+$

b) diffusione
B (p-type)



$1\mu\text{m}$
termico

c) PLANAR
heating - 1000°C



d) impiantazione
heating 700°C

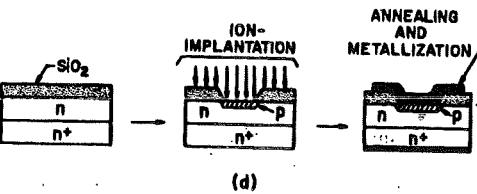
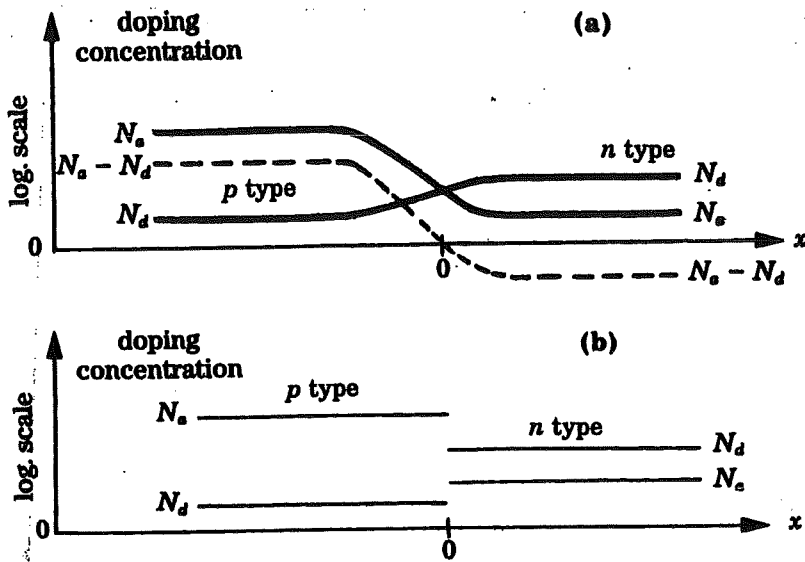


Fig. 1 Some device fabrication methods. (a) Alloyed junction. (b) Diffused mesa junction. (c) Diffused planar junction on epitaxial substrate. (d) Ion implantation.

GIUNZIONE p-n



⇒ Modello di Schottky

Fig. 8.2. Doping profile of a p-n junction: (a) real profile; (b) approximation as a discontinuous profile.

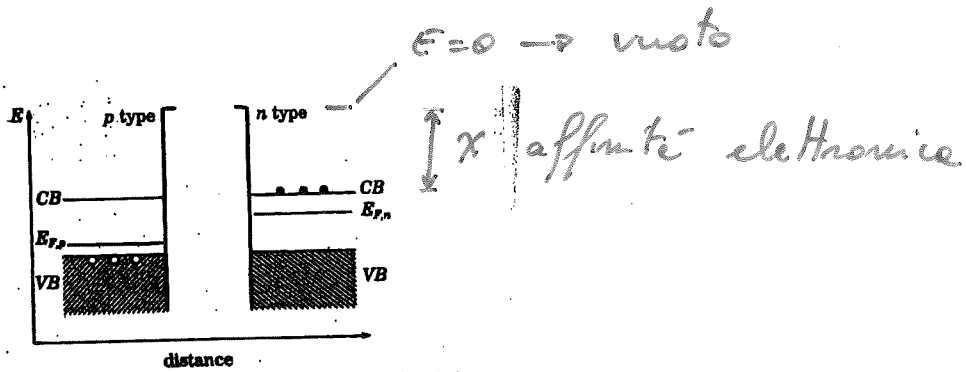
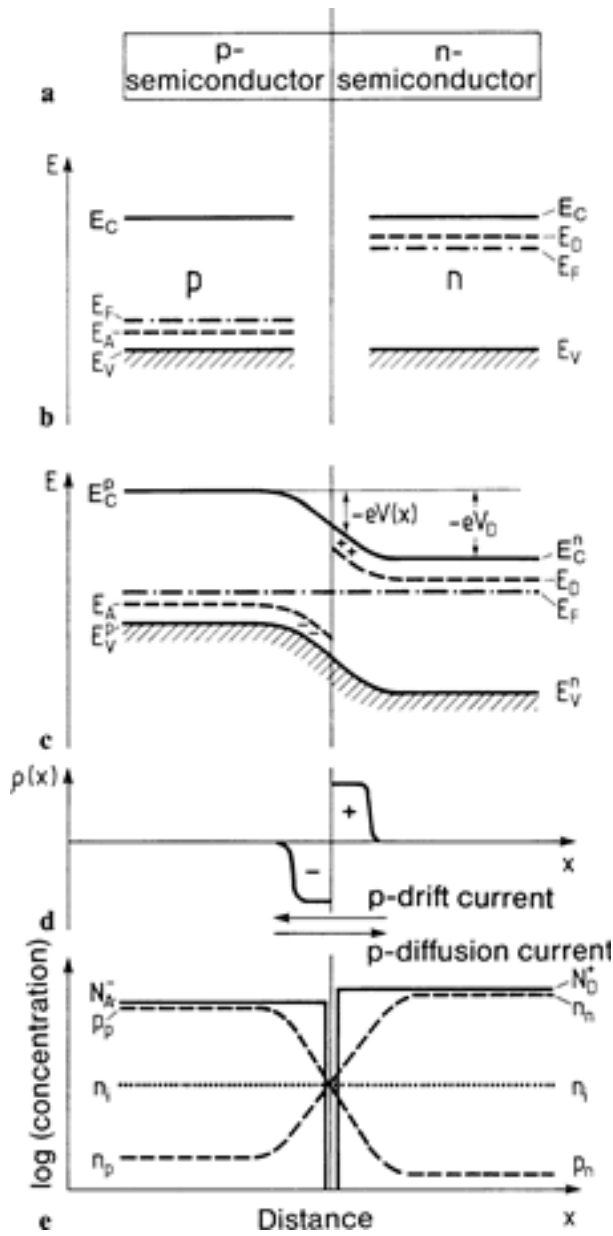


Fig. 8.3. Energy levels in two separated n- and p-type crystals. The hatched zones represent filled states, the heavy dots conduction electrons, and the open dots holes. (After Dalves, "Introduction to Applied Solid State Physics," Plenum Press, 1980.)



See p 74

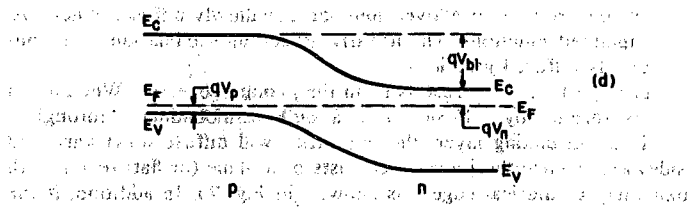
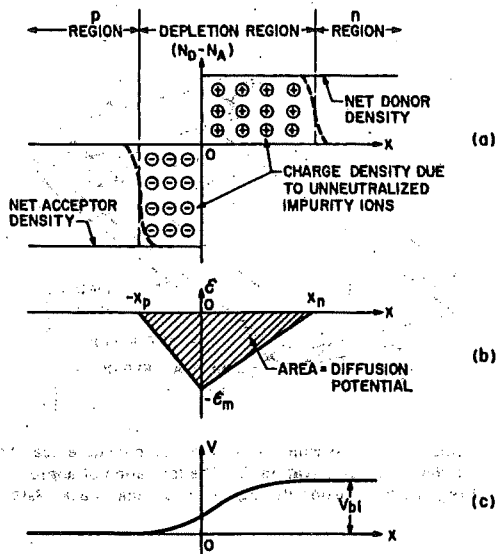


Fig. 10 Abrupt p-n junction in thermal equilibrium. (a) Space-charge distribution. The dashed lines indicate the majority-carrier distribution tails. (b) Electric field distribution. (c) Potential variation with distance where V_{bi} is the built-in potential. (d) Energy band

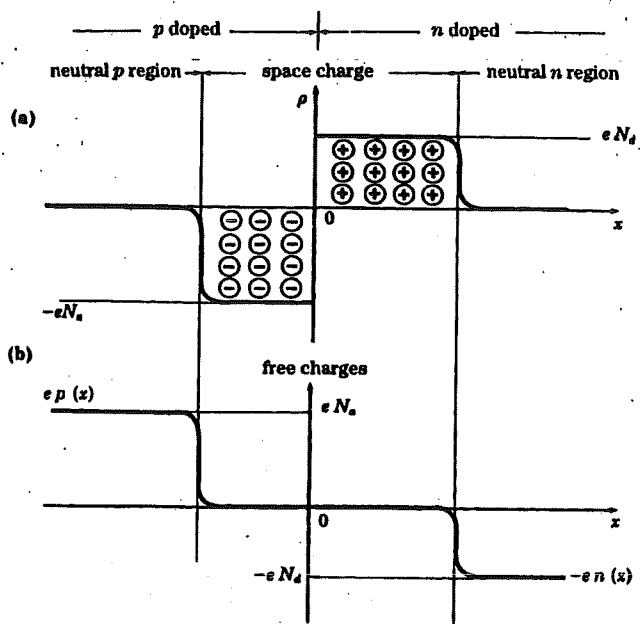
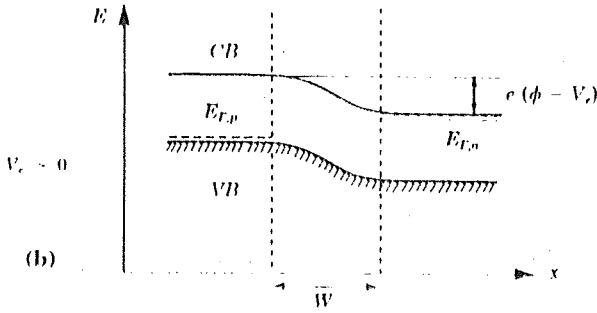
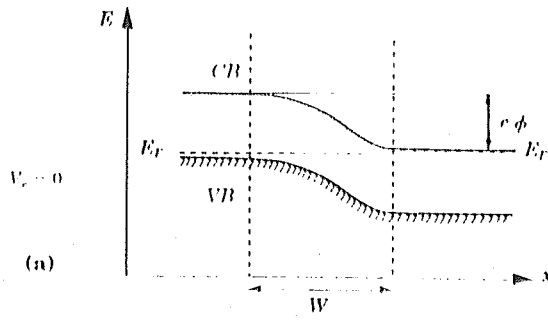


Fig. 8.4. (a) Net charge density $\rho(x)$, and (b) free charge density, in a p-n junction.

Densità di cariche
totali

Densità di portatori
liberi



Pol. diretta

Pol. inversa

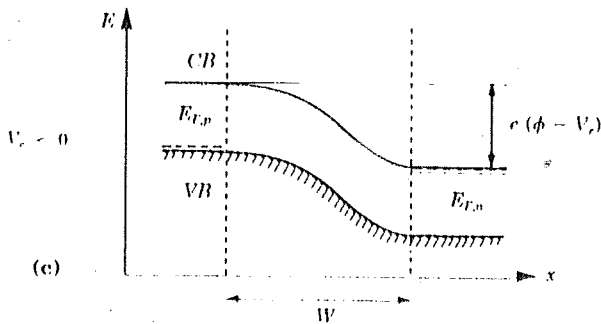
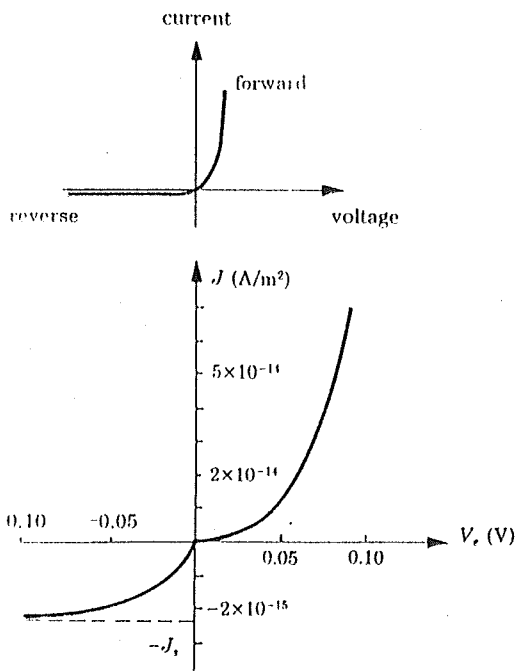


Fig. 8.9. Comparison of band profiles for a p-n junction which is (a) unbiased; (b) forward biased; and (c) reverse biased.



$$J = J_s \left[e^{\frac{eV_e}{kT}} - 1 \right]$$

$$J_s = e n_i^2 \left(\frac{D_e}{L_e N_a} + \frac{D_n}{L_n N_d} \right)$$

Fig. 8.10. Current-voltage characteristic of a p-n junction. (a) Linear scale; (b) enlarged view of the region near the origin. The current density scale is expanded by a factor 10 for the reverse region, causing the change of slope at the origin.